Journal of Electronics and Informatics (ISSN: 2582-3825)
www.irojournals.com/iroei/

# Design and Analysis of an Extruder for Bio-Composite Filament Fabrication

**R. Vinodhkumar[1], T. Sekar[2], N. Nandakumar[3]**

[1,2,3]Department Of Mechanical Engineering, Government College Of Technology, Anna University, Coimbatore, Tamil Nadu, India

**E-mail:** [1]vk1809569@gmail.com, [2]drtsekar76@gct.ac.in, [3]nandakumar@gct.ac.in

## Abstract

Fused Deposition Modelling (FDM) or Fused Filament Fabrication (FFF) is an additive manufacturing technique in which layers of materials are fused together in a pattern to form an item. Acrylonitrile Butadiene Styrene (ABS), Poly Lactic Acid (PLA), Poly Ethylene Terephthalate (PET), Poly Vinyl Alcohol (PVA), Sandstone, and other materials are utilised in this FDM 3D printer. However, the rapid changes of Global needs and advances in Engineering domain, are in need of the combination of new materials to cater to fulfil the society and technical demands. Therefore, this work attempts to develop a new bio-composite filament for making components, which are associated with medical application. The commercially available extruders are not so cost effective and custom based for the biomaterials chosen for this work.

The selected materials for making the bio-composite are Poly Lactic Acid (PLA), Ultra High Molecular Weight Poly Ethylene (UHMWPE) along with Cissus quadrangularis (Adamant creeper) powder. So, it is essential to design and develop an extruder indigenously to make the Bio-composite filament. For this first phase, the basic components of the customized designed extruder are modelled using Solidworks 2018 and assembled. Subsequently the usage viability analysis is done by using ANSYS 18.1 at Manufacturing Engineering CAD laboratory. The thermal and dynamic analysis are successfully carried out. The results reveal that the heat sink of extruder could withstand up to $300^0$C and the heat transfer rates are reported.

**Keywords:** Fused Deposition Modelling, Poly Lactic Acid, Ultra High Molecular Weight Poly Ethylene, Cissus quadrangularis.


*DOI: https://doi.org/10.36548/jei.2022.1.005*
*Received: 18.03.2022, received in revised form: 09.04.2022, accepted: 24.04.2022, published: 04.05.2022*

## 1. Introduction

By adding material to a geometrical representation, 3D printing may build tangible items. In recent years, this 3D method has seen tremendous growth. It offers up new options and provides enterprises hoping to increase their production efficiency fresh hope. The use of 3D printing technology will speed up manufacturing while also lowering expenses. At the same time, consumer demand will have a greater impact on manufacturing. Jayant Giri et al. (2021) explained how essential process parameters including layer thickness, air gap, raster width, build orientation, raster angle, and the number of contours are tuned to improve FDM printed product attributes like tensile strength, surface roughness, and build time.

Polylactic acid is the substance utilised in 3D printing (PLA). Using function approximation of Artificial Neural Networks, the process of training and optimising the data sets was completed. For tensile strength, construction time, and surface roughness, ANN can predict experimental data with R = 0.9981,0.9984,0.99837 and root mean square error of 0.5543, 0.578, and 0.241 for three outputs, respectively. The different parts design and assembly utilised in FFF 3D printers were documented by Keishnanand et al. (2021).

Theoretical and technical details of different mechanical and electronic accessories or components, as well as software needs for FFF 3D printers, are offered in order to realise this. This good functioning of the FFF 3D printer and future directions to lower energy consumption by enabling appropriate and viable integration of pallet and filament powered solid based 3D printing technologies. The inlet and outlet angles, as well as the throat length, have been mathematically evaluated by Mantu Choudhary et al. (2021)to showed that there are ideal values for all three geometrical parameters in order to achieve the largest air flow velocity at the output, and that flow behaviour degrades beyond these optimum values.

According to the numerical study, a 20° outlet angle, 3 mm throat length, and 40° intake angle optimised convergent-divergent duct may boost the average air flow velocity by roughly 23% over a typical component cooling fan without the convergent-divergent section. J.m. Jafferson et al. (2021) conducted a finite element numerical simulation of heat transmission in the filament extruder of a 3D printer with different new cooling fin design configurations, finding that square fins provide the lowest temperature among the four types of heat sinks. Due to form index, the hexagonal shape perforation geometry produced the lowest temperature of all the square perforated designs.

Different properties of 3-D printed materials were simulated by Bimal Kumar Mawandiya et.al (2021), so that it may be utilised whenever needed with exact information. The authors looked at resolution, printed strength, and print pattern as input factors, while diverse experiments including tensile testing, impact testing, absorption testing, porosity measurement testing, and dielectric strength measurement were performed as output parameters.

Based on the results of the testing, it may be inferred that specific input parameters are the optimal combination for specific applications and should be set. Jianning Tangetal. (2021) proposed an in-orbit 3D printing device that can operate at temperatures up to 400 ° C in a vacuum environment. To verify the feasibility of on-orbit manufacturing, four extruders with different characteristics were designed. The heat transfer model was used to examine the temperature profile of the entire extruder under vacuum conditions. Based on thermal analysis, thermal control methods have been developed that combine Strategic Proportion (P) and Fuzzy Proportion and Integration (Fuzzy PI) to coordinate the behaviour of 3D printing devices.

Check the melting and solidification state of PEEK (poly ether ether ketone) material at an extrusion speed of 8654.6 mm3 / h and a pressure of 400 ° C. Ral Vallejos Baier et al. (2021) is low by producing solid and porous samples using suitable microarchitectures in the physiological range (pore size of 100-500 μm) and comparing them with commercially available ones. Evaluated cost / open-source 3D printer (In House). For microarchitecture studies, we compared pore size and porosity values with the corresponding computer-aided design (CAD) models in samples from both printers. By comparing FEA and CAD models, in-house printers typically achieved better mechanical behaviour and better resolution than comparable printers on the market.

The effect of pore shape on the mechanical properties of 3D scaffolds. It shows that parameters such as apparent modulus (Eapp) can be adjusted with a 3D printed scaffold. Ibrahim Mrani et al. (2021) described thermoplastic filaments made out of granules, pellets, and waste plastic components. This approach addresses these concerns while also improving mechanical qualities. The mechanical qualities of filament achieved in our manufacture will be deemed good. Time and money have been saved. Diana Gregor-Svetec et al. (2020) investigated HDPE composites manufactured with various weight percent of cardboard dust, i.e., a by-product of corrugated box manufacturing. The technical, mechanical, and dynamic

mechanical characteristics of HDPE composite filament with 20% cardboard dusts suggest a viable way to obtaining filaments for use in the FDM process.

## 2. Project Gap Identified

Rapid changes in global needs and advances in engineering require new combinations of materials to meet social and technical demands. Therefore, this task attempts to develop a new bio composite filament for manufacturing components related to medical applications. Commercially available extruders are not cheap and custom made for the biomaterial selected for this task. The materials selected for the production of bio composites are Polylactic Acid (PLA), Ultra-High Molecular Weight Polyethylene (UHMWPE), and Cissus quadrangularis (Adamant Creeper) powder. Therefore, it is important to design and develop your own extruder for manufacturing bio composite filaments.

The aluminium used in Heat sink and heat block is replaced by PolyEther Ether Ketone (PEEK) for withstanding temperature of bio composite filament fabrication.

### 2.1 Materials Selection & Experimentation

To withstand temperature for bio composite filament fabrication, the conventional Aluminium material was replaced by PolyEther Ether Ketone (PEEK).

### 2.2 PolyEther Ether Ketone (PEEK)

PEEK is a high-performance designed polymer with one of the best strength-to-weight ratios of any thermoplastic and outstanding heat tolerance. Glass, steel, aluminium, and other polymers can all be replaced with PEEK. For difficult applications, the material's strength is complimented by its high purity and smoothness. PEEK can keep rigidity at high temperatures and is appropriate for continuous usage at temperatures above 300 ° C. This engineering plastic has a proven track record in demanding applications including aerospace, oil and gas, food and beverage processing, and semiconductor manufacturing.

**Table 1.** Properties of PEEK

| Property | Values |
|---|---|
| Dielectric Strength | 20(kV/mm) |
| Elongation at Break | 30 – 150(%) |

| | |
|---|---|
| Young Modulus | 3.5 - 3.9(GPa) |
| Toughness (Notched Izod Impact at Room Temperature) | 80 – 94(J/m) |
| Density | 1.26 - 1.32($g/cm^3$) |
| Thermal Insulation (Thermal Conductivity) | 0.25(W/mK) |

## 2.3 Materials for Bio-Composite Filaments

Materials used in this bio composite filaments are Poly Lactic Acid (PLA), Ultra High Molecular Weight Poly Ethylene (UHMWPE) along with Cissus quadrangularis (Adamant creeper) powder.

## 2.4 Filaments Made of Bio-Composites

Composite filaments are made up of many materials. In most situations, a powdered solid is embedded in a plastic matrix. The plastic matrix permits the composite material to function similarly to any plastic filament, with the most crucial difference being that the filament keeps its thermosetting capabilities. Most plastic filaments have 60 percent to 70 percent plastic material and 30 percent to 40 percent solid powder.

The following materials are Poly Lactic Acid (PLA), Ultra High Molecular Weight Poly Ethylene (UHMWPE), and Cissus quadrangularis (Adamant creeper) powder.

## 2.5 Poly Lactic Acid (PLA)

PLA is a bio plastic, used in 3D printing using the FDM (Fused Deposition Modelling) is one of the standard materials for this technology. There is often a tendency to compare these plastic materials, as they are the two most common alternatives available for consumer printers. PLA plastic material is easy-to-use and offers some interesting mechanical properties.

## 2.6 Ultra High Molecular Weight Poly Ethylene (UHMWPE):

Ultra-High Molecular Weight Poly Ethylene (UHMWPE) is distinguished by non-toxicity, a simple chemical composition and structure, minimal water absorption, and chemical and radiation resistance. UHMWPE has a lower friction coefficient than steel, good

wear resistance (including abrasion), and substantial impact toughness, all of which are required in biomedical applications.

### 2.7 Properties Of UHMWPE and PLA

**Table 2.** Properties of PLA and UHMWPE

| Properties | UHMWPE | PLA |
|---|---|---|
| Density | 0.95 g/$cm^3$ | 1.24 g/cm³ |
| Tensile strength | 40 MPa | 50 MPa |
| Specific heat | 1.84 J/gK | 1.8 J/gK |
| Coefficient of thermal conductivity | 0.41 W/mk | 0.12 W/mk |

### 2.8 Cissus Quadrangularis

The common names for Cissus quadrangularis include veldt grape, devil's backbone, adamant creeper, Asthisamharaka or Asthisamhara, Hadjod, and Pirandai. Cissus quadrangularis is now employed in a range of therapeutic applications such as bone tissue, bone setting, scaffolds, and so on.This plant's principal ingredients are ascorbic acid, triterpene, -sitosterol, ketosteroid, two asymmetrical tetracyclic triterpenoids, and calcium.

## 3. Design and Modelling

### 3.1 Heat Sink

The heatsink constitutes the bulk of the coldside or cooling system for the hotend. It functions as a heat exchanger, diverting heat away from the filament route. Poly Ether Ether Ketone replaces aluminium in this case to withstand temperature. Figure 1 shows that the Drafted view include Top view, Bottom view, side view and Front view of Heat sink with dimensions. The figure 2 shows 3D model of Heat sink drawn on Solidworks 2018.

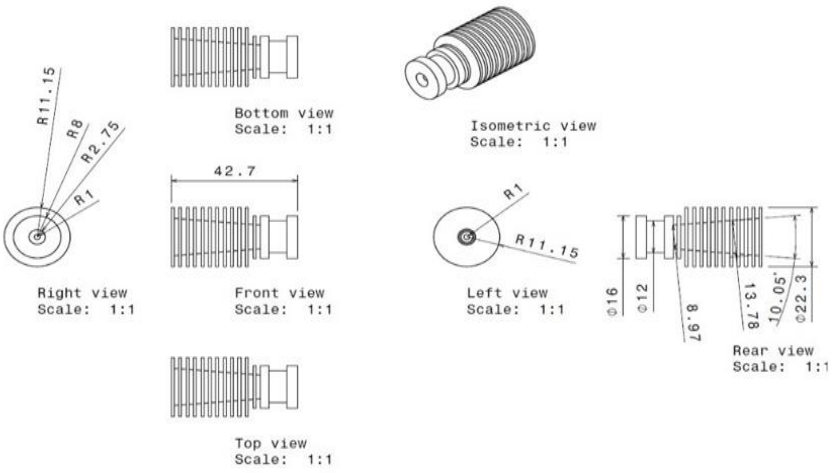


**Figure 1.** Dimensions of Heat Sink

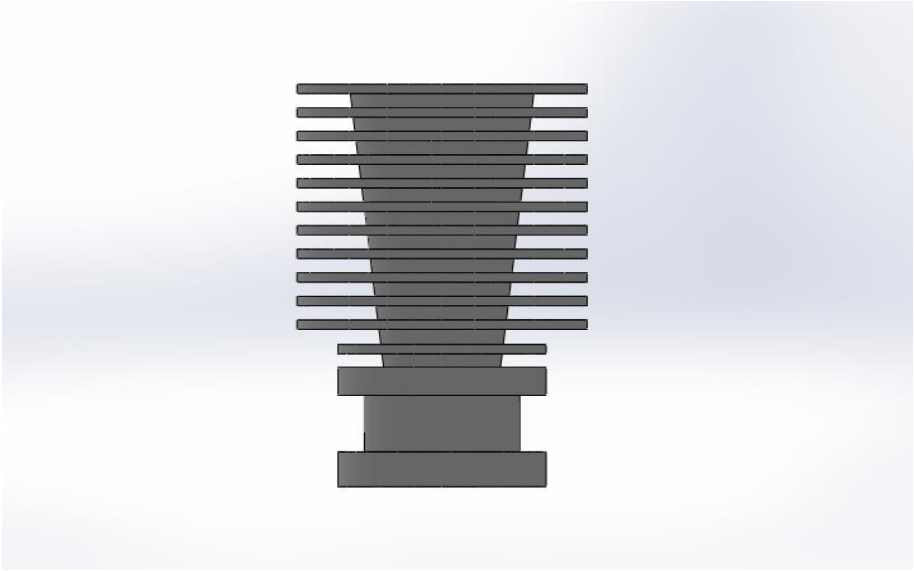

**Figure 2.** Solidworks Model of Heat Sink

### 3.2 Heat Block

The Heatblock is in charge of mechanically and thermally connecting the heater, sensor, and nozzle to form a single collaborative system. Perhaps more crucially, the Heatbock serves as a heat reservoir for the nozzle, keeping its temperature steady and reducing thermal fluctuations.

Figure 3 shows that the Drafted view include Top view, Bottom view, side view and Front view of Heat block with dimensions.

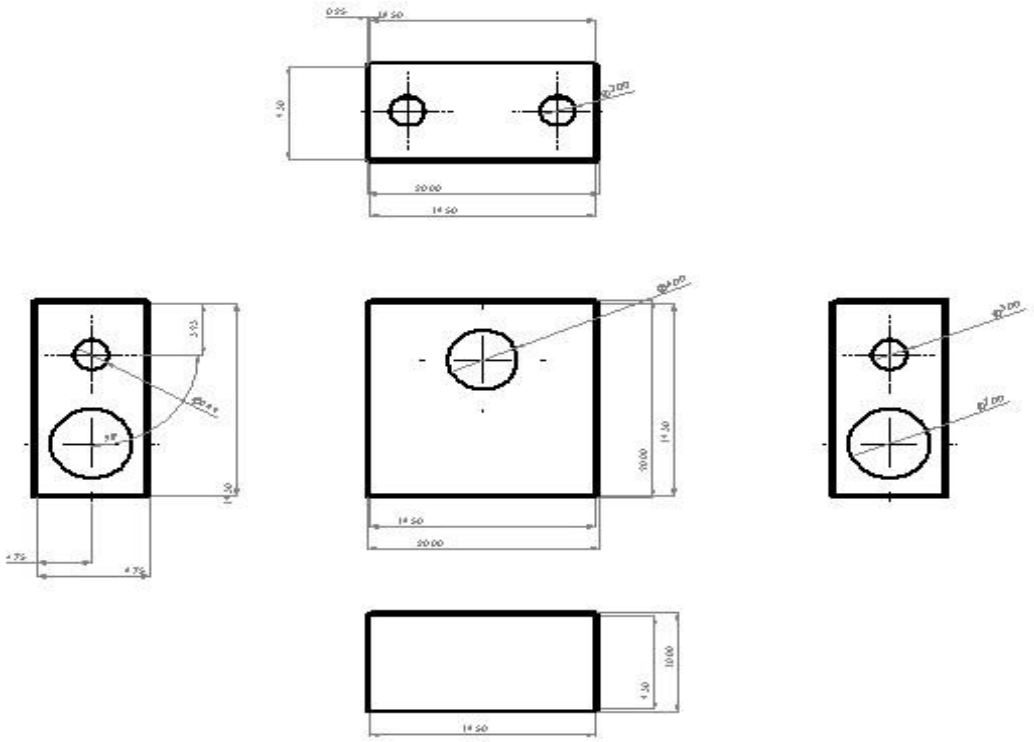

**Figure 3.** Dimensions of Heatblock

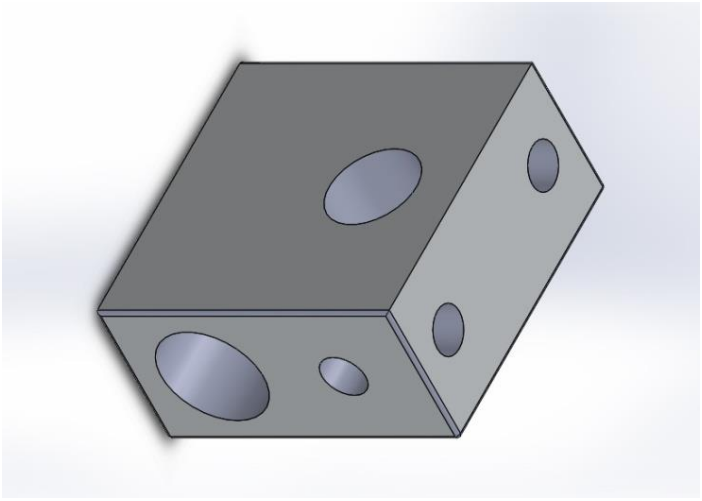

**Figure 4.** 3D Solidworks Model of Heat Block

The above figure 4 shows 3D model of heat block drawn on Solidworks 2018.

### 3.3 Heat Break

The HeatBreak is a threaded metal tube that mechanically secures and thermally separates the cold and hot sides of the HotEnd.

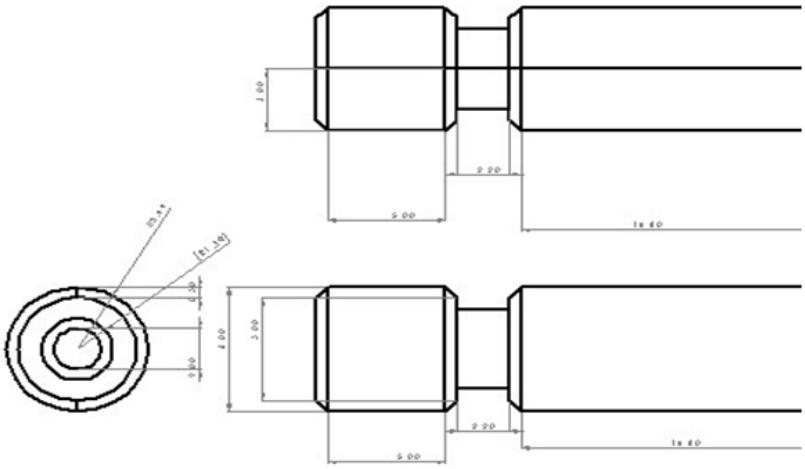

**Figure 5**. Dimension of Heatbreak

Figure 5 shows that the Drafted view include Top view, Bottom view, side view and Front view of Heat break with dimensions.

**Figure 6.** Solidworks Model of Heat Break

The above figure 6 shows 3D model of heat break drawn on Solidworks 2018.

### 3.4 Teflon Tube

A PTFE liner in certain hotends guides the filament through the heat break and into the nozzle. This makes PLA printing easier, but also restricts the temperatures at which you can print when compared to an all-metal hotend.

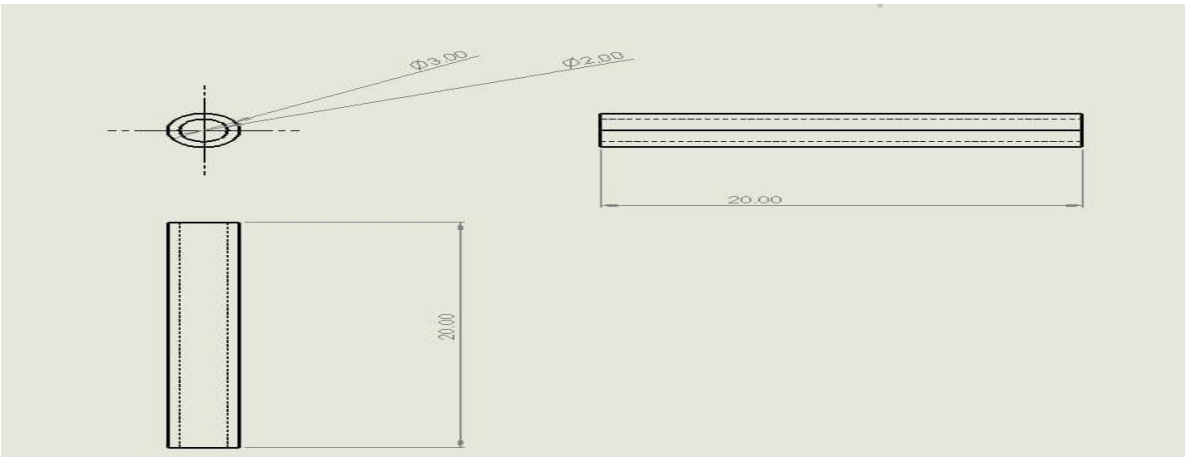


**Figure 7.** Dimension of Teflon Tube

Figure 7 shows that the Drafted view include Top view, Bottom view, side view and Front view of Teflon tube with dimensions

**Figure 8.** Solidworks Model of Teflon Tube

The above figure 8 shows 3D model of teflon tube drawn on Solidworks 2018.

### 3.5 Nozzle

The nozzle is the final component of our Hotend; its internal geometries are perfectly oriented to facilitate optimal flow from its opening and prevent blockages; its outward geometries are equally critical.

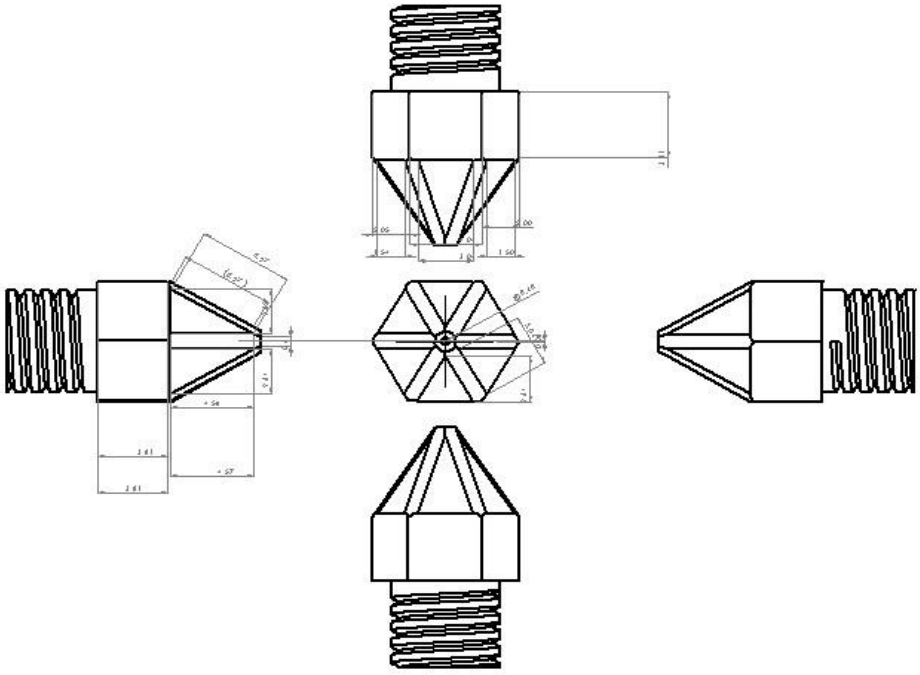

**Figure 9.** Dimensions of Nozzle

Figure 9 shows that the Drafted view include Top view, Bottom view, side view and Front view of nozzle with dimensions

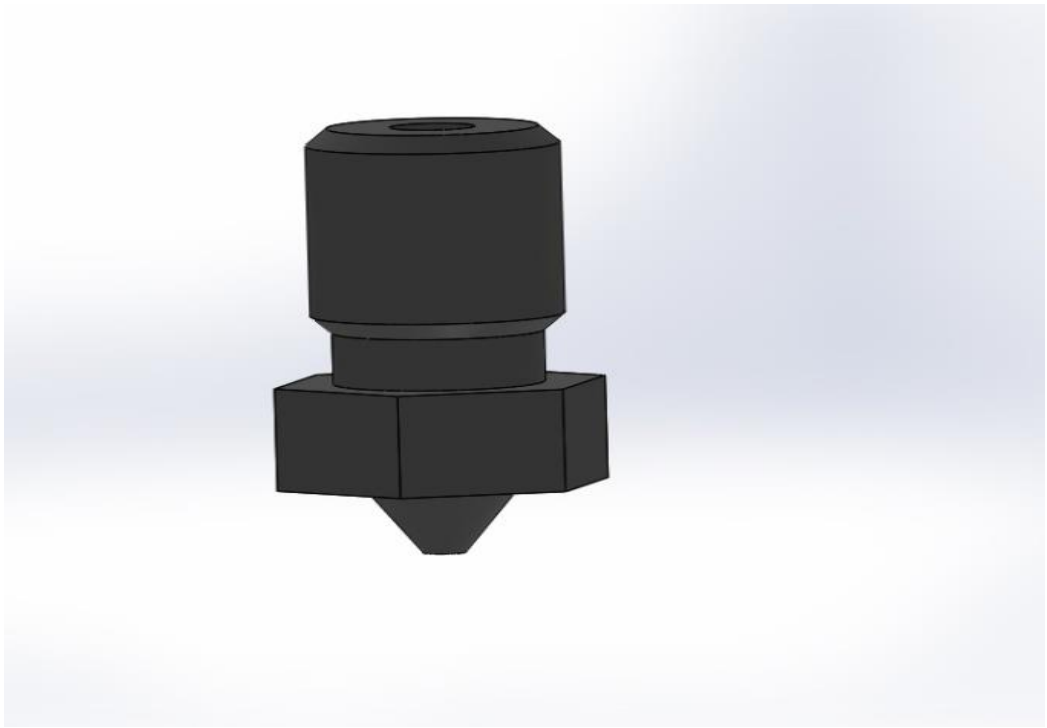

**Figure 10.** Solidworks Model of Nozzle

The above figure 10 shows 3D model of Nozzle drawn on Solidworks 2018.

### 3.6 Assembled Part

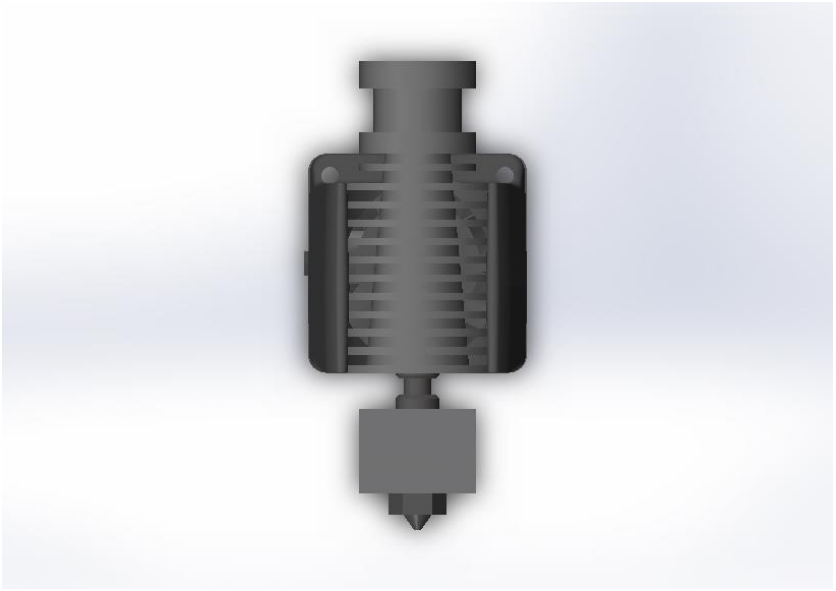

**Figure 11.** Assembled Model of Hotend

The above Figure 11 shows that assembled part of Extruder done on solidworks assembled part. Assemble part includes Heat block, Heat sink, Teflon tube, Heat break and Nozzle.

## 4. Result and Discussion

### 4.1 Thermal Analysis

Thermal analysis is a broad phrase that refers to a technique for determining the time and temperature at which physical changes occur when a substance is heated or cooled.

### 4.2 Total Heat Flux of Heatsink

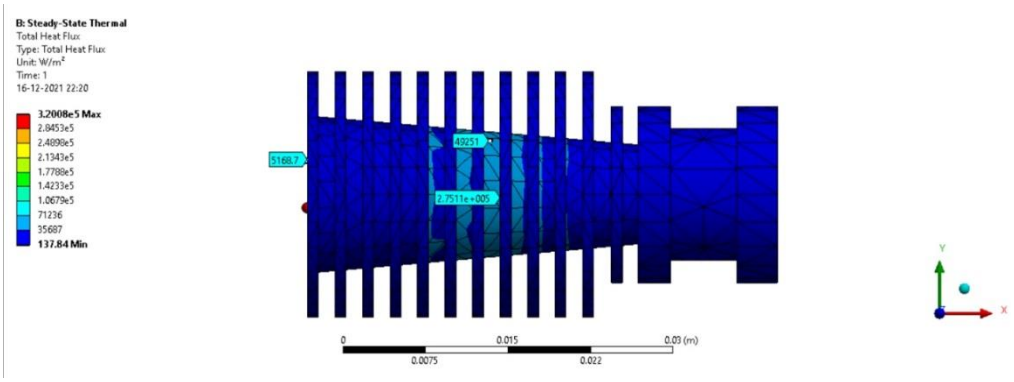


**Figure 12**. Total Heat flux of Heatsink

The energy per unit time is defined as the heat flow rate in heat transfer. Heat flux has the unit of W/$m^2$. The above figure 12 shows that side view of Heat flux transferring into heat sink. Heat Sink at middle of Heat sink is 2.7511*$10^5$W/$m^2$ and remaining are minimum Heat Flux.

### 4.3 Total Heat Flux for Top of Heatsink

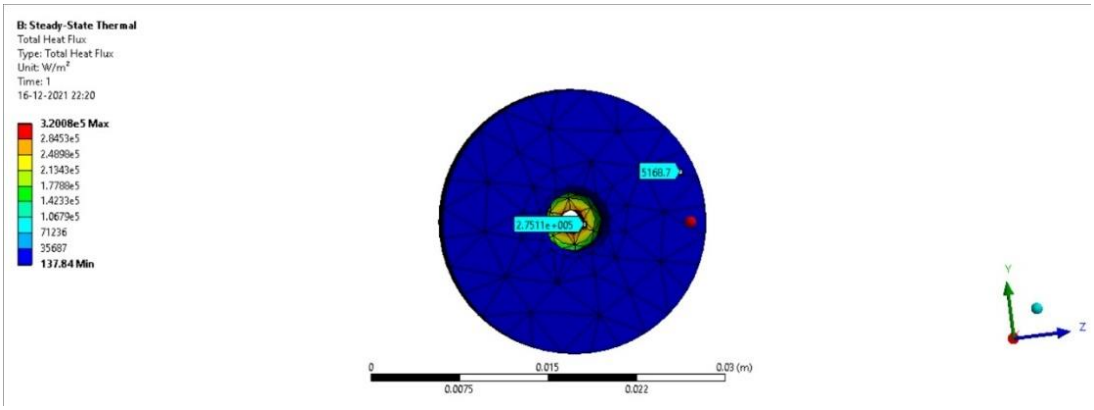


**Figure 13.** Total Heat Flux for Top of Heatsink

The above figure 13 shows that top view of Heat flux transferring in to Heat sink. Heat Sink at centre of Heat sink is 2.7511*$10^5$ W/$m^2$ and remaining are minimum Heat Flux.

### 4.4 Temperature at Top of Heatsink

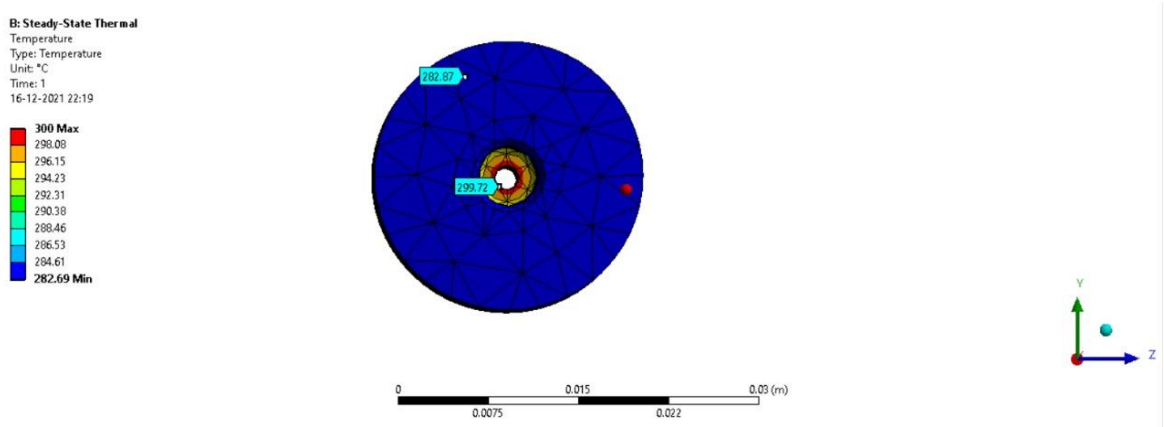


**Figure 14.** Temperatures at Top of Heatsink

Temperature distribution is the rate of change of temperature with displacement in a given direction. Here the figure 14 shows temperature at top of heat sink. The temperature distribution at middle of heatsink about 299.72$^0c$.

## 4.5 Temperature at Heatsink

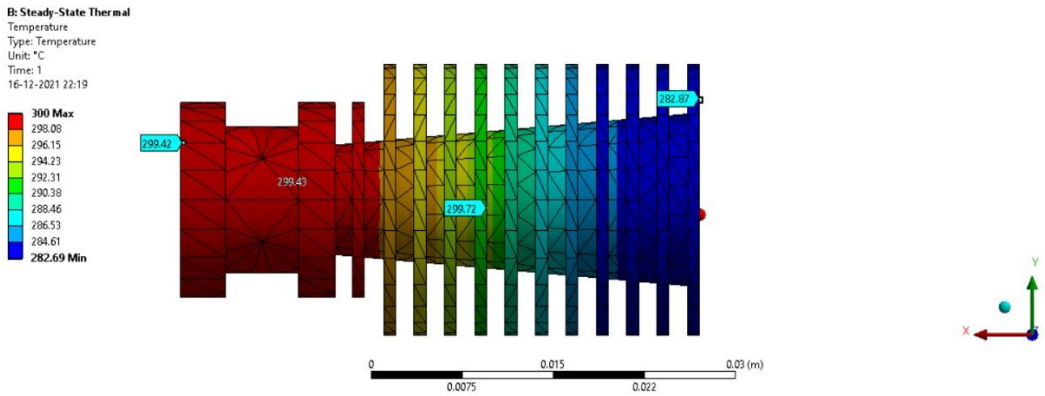


**Figure 15.** Temperatures at Heatsink

Here the figure 15 shows temperature at outer side of heat sink. The temperature distribution at middle of heatsink about $299.72^0c$, at top $299^0c$ and at bottom $282.87^0c$ .

## 4.6 Directional Heatflux of Heatsink

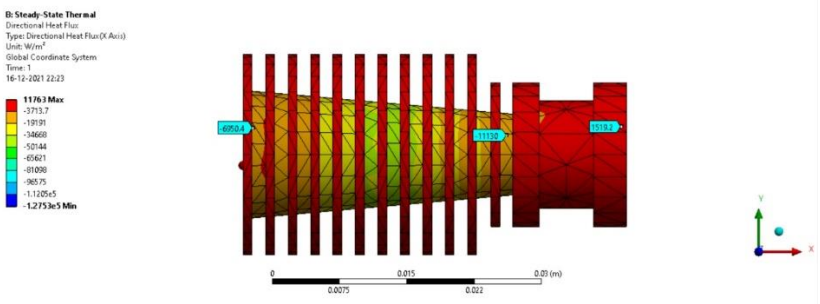


**Figure 16.** Directional Heat flux of Heatsink

The figure 16 shows directional heat flux of Heatsink. The Heat flux is maximum at near the heat block about 1519.2 W/$m^2$ .

## 4.7 Total Heat Flux of Extruder Hotend

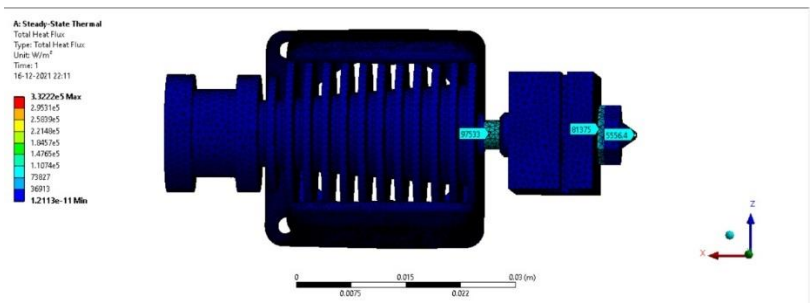


**Figure 17.** Total Heat Flux of Extruder Hotend

The figure 17 shows directional heat flux of Extruder Hotend. The Heat flux is slightly at near the Teflon tube about 97553 W/$m^2$ and 5556.4 W/$m^2$ near the nozzle.

## 5. Conclusion

In this project, Extruder is designed indigenously to make the bio-composite filament, and analysed to ensure a better heat concentration in the area of the Heatsink and Nozzle, avoiding as much as possible dissipation of heat to the 3D printer frame or to the environment. Lowering the temperature of the material passage, improves the sliding of the material, because it is heated only in the area of extrusion, where it is needed. The FEA thermal analysis confirmed that the temperature measured on the nozzle is sufficient to melt the PLA (melting temperature 200°C), UHMWPE (melting temperature 152°C) along with CISSUS QUADRANGULARIS (Adamant creeper). Furthermore, the temperature value of the modified extruder could withstand up to $300^0\ C$.

## References

[1] Giri, Jayant, Pranay Shahane, Shrikant Jachak, Rajkumar Chadge, and Pallavi Giri. "Optimization of FDM process parameters for dual extruder 3d printer using Artificial Neural network." Materials Today: Proceedings 43 (2021): 3242-3249.

[2] Ilo bodi, luigi m. Galantucci, jorgaq kacani, erald piperi (2017). Extruder head thermal analysis for an open-source 3D printer December 2017 Conference: International Conference Engineering and Entrepreneurship 2017. https://www.researchgate.net/publication/321585844.

[3] Taoufik Hachimia, Nassima Naboulsia, Fatima Majida, Rajae Rhanimb, Ibrahim Mrania, Hassan Rhanima (2021). Design and Manufacturing of a 3D printer filaments extruder. IGF26 - 26th International Conference on Fracture and Structural Integrity https://creativecommons.org/licenses/by-nc-nd/4.0.

[4] R. Jerez-Mesa, J. A. Travieso-Rodriguez, +2 authors G. Gómez-Gras (2016). Finite element analysis of the thermal behavior of a RepRap 3D printer liquefier DOI: 10.1016/J.MECHATRONICS.2016.04.007.

[5] Abubaker Nooralhoda Ahmed Altayeb (2020). Build Low-Cost 3D Delta Printer using Fused Deposition Modeling Technology. Volume 09, Issue 02 http://dx.doi.org/10.17577/IJERTV9IS020047.

[6] Sathies, T., P. Senthil, and M. S. Anoop. (2020). A Review on Advancements in Applications of Fused Deposition Modelling Process. Rapid Prototyping Journal 26 (4): 669–87. http://dx.doi.org/10.1108/RPJ-08-2018-0199].

[7] Foresti, Ruben, Stefano Rossi, and Stefano Selleri. (2019). Bio-Composite Materials: Nano-Functionalization of 4D Bio-Engineered Scaffold. IEEE International Conference on Bio Photonics (Bio Photonics) 100–101. https://doi.org/10.1109/ICB47650.2019.8945042.

[8] Attaran, Mohsen. (2017). The Rise of 3-D Printing: The Advantages of Additive Manufacturing over Traditional Manufacturing. Business Horizons 60 (5): 677–88. 10.1016/j.bushor.2017.05.011.

[9] Huang, Samuel H., Peng Liu, Abhiram Mokasdar, and Liang Hou. (2013). Additive Manufacturing and Its Societal Impact: A Literature Review. International Journal of Advanced Manufacturing Technology 67 (5–8): 1191–1203.

[10] Holzmann, Patrick, Robert J. Breitenecker, Aqeel A. Soomro, and Erich J. Schwarz. (2017). User Entrepreneur Business Models in 3D Printing. Journal of Manufacturing Technology Management 28 (1): 75–94.